EBIC Characterization and Hydrogen Passivation in Silicon Sheet

Jack I. Hanoka
Mobil Solar Energy Corporation
Waltham, Massachusetts 02254

ABSTRACT

As a general qualitative tool, the electron beam induced current (EBIC) method can be very useful in imaging recombination in silicon sheet used for solar cells [1,2]. In this paper, work using EBIC on EFG silicon ribbon will be described. In particular, some efforts at making the technique more quantitative and hence more useful, some limitations of the method, and finally specific application to hydrogen passivation will be treated. As an introduction, some brief remarks will be made regarding the technique itself.

The EBIC Technique

Figure 1 shows a schematic of the EBIC process. An electron beam impinges on a semiconductor sample containing a junction of some sort. The energy of the electrons in the beam typically ranges from 1 to 50 keV while the minimum energy to create hole-electron pairs in a semiconductor is the band gap, which is on the order of 1 eV. As a result, a single high energy electron incident on the semiconductor produces many hole-electron pairs, on the order of 10^3 to 10^4 per incident electron. The electron-hole pairs are created within the material in a volume termed the generation volume. The important carriers here are the minority carriers -- electrons in the p-type layer and holes in the n-type layer. If the diffusion length of the generated minority carriers is long enough, they will diffuse to the p-n junction and be swept across it by the strong field present, thus producing a current that can be measured externally. This is the electron-beam-induced current. This current can then be amplified even further and the amplified signal used to drive the CRT display of the SEM, while it is scanned synchronously with the electron beam. The result is a mapping of the current collected at every scanned point. If a defect such as a grain boundary or a dislocation is present, the resulting recombination at such a defect will produce less collected current and a darker image (corresponding to less current collection) in the CRT display. Examples of EBIC images of recombination at grain boundaries and at dislocations will be shown in later figures in this paper.

The description above indicates that EBIC is an electron-beam analog of the photovoltaic effect. The images one obtains using light beam induced current (LBIC) are, in fact, similar to those seen from EBIC. LBIC generally has poorer resolution than EBIC but offers the ability to generate carriers at varying distances according to the wavelength of the light chosen.

With EBIC, the depth of penetration or the range R, of the electron beam is a function of the electron beam energy, E, with this form for silicon:

$$R = (0.032)\ E^{1.67} \qquad (1)$$

where R is in microns and E is in keV. The range-energy relation depends on the model chosen, another commonly used model gives R ~ 7 μm at 30 keV [1].

A reasonable and useful approximation for silicon is to consider the electron-hole pair generation volume to be a sphere tangent to the sample surface. R is then the diameter of this sphere. For a 30 keV beam, R ~ 9 μm. R is also a measure of the resolution obtainable. It is important to note that the resolution is only weakly dependent on the minority carrier diffusion length and is mainly determined by the value of R.

There is a considerable body of literature now available on quantifying EBIC, but we will concern ourselves with two or three techniques in particular which we have found useful in studying solar cells.

Low Temperature EBIC

As mentioned above, an EBIC image provides a recombination map. In addition to simply knowing the spatial location of recombination sites, it is important, particularly from the point of view of making higher efficiency silicon ribbon solar cells, to further understand what is taking place at these recombination sites.

Accordingly, we have investigated the use of EBIC at low temperatures [3]. In general, a considerable amount of recombination contrast enhancement is seen in EFG ribbon silicon when going from room temperature to, say, 200°K. Through the use of a trapping model, it was shown that the experimental results obtained could be interpreted as due to shallow energy states located below the conduction band and that the activation energy of these levels could be calculated from the low temperature EBIC data.

Furthermore, the behavior of these traps as a function of thermal processing and $[O_i]$ has been studied and will be discussed below.

The ribbon samples studied here were p-type, with ρ ~ 1 Ω-cm. Both Al Schottky barriers and PH_3 diffused junctions were used as collecting junctions for the EBIC work. The low temperature EBIC was done using a liquid nitrogen-cooled specimen mount which was fitted to a Cambridge S4-10 SEM. The ribbon sample and a single crystal CZ reference sample were mounted on a thick copper block with a thermocouple between the two samples. With this arrangement, the electron beam induced current at a particular defect could be measured by adjusting the condenser lenses on the SEM to give a pre-selected value of the EBIC for the CZ reference cell. No significant defects were observed in the CZ reference cell at 300°K or down to 200°K. An assumption used in making the measurements is that the EBIC of the reference cell is independent of temperature.

The general result observed is shown in Fig. 2 where the enhanced recombination along and between the linear boundaries at low temperature can readily be seen. In the room temperature photograph in Fig. 2 (top photograph), the prototypical defects seen by EBIC on EFG ribbon are evident. These are linear boundaries parallel to the growth direction and arrays of dislocations

within bands bordered by linear boundaries.

Quantifying the above is done by measuring the EBIC signal at a particular defect as a function of temperature. Using the single crystal reference cell and the value of the EBIC signal at the defect, a diffusion length L, could be assigned to the region enclosing the defect [3,4].

A model was developed in which the enhanced recombination seen at lower temperatures was viewed as due to trapping of electrons at shallow levels below the conduction band [3]. Figure 3 shows the scheme used for the model. If such a level is at an energy ΔE below the conduction band, then it was possible to show that

$$L^2 T^{1/2} \propto e^{-\Delta E/kT} \qquad (2)$$

Thus, measuring the value of L at a particular defect as a function of temperature would permit the calculation of the trap activation energy, ΔE. In this way, three shallow traps were found, E_c - 0.04 eV, E_c - 0.10 eV, and E_c - 0.13 eV.

The behavior of these traps indicates considerable sensitivity to both the particular growth conditions (quartz or graphite crucibles), addition or non-addition of CO_2 to the growth ambient used, and also to the temperature employed for the n-type diffusion.

A feature common to all the above cases is the spatial anchoring of these traps at dislocations or at linear boundaries. The location of these traps is not affected by diffusion temperatures up to 1050°C, at least within the EBIC spatial resolution limit of ~9 μm for a 30 keV electron beam. Figures 4 and 5 illustrate some differences in EBIC temperature behavior (increasing recombination with decreasing temperature) for the as-grown quartz crucible and as-grown graphite crucible silicon ribbon. The graphite material (Fig. 5) shows a saturation at temperatures below 153°K indicating that below this temperature electrons do not detrap back into the conduction band but undergo a transition to a deeper level at which recombination takes place. This latter process takes place with relatively little temperature sensitivity as opposed to the exponential behavior of the detrapping process. The quartz-grown material (Fig. 4), on the other hand, shows either no saturation down to 140°K or the trap distribution changes at ~188°K from the 0.04 level to a dominance of either the 0.10 level or the 0.13 level.

Trap behavior in solar cells made from the graphite crucible material in which the $[O_i]$ was varied by changing the CO_2 partial pressure in the growth ambient showed a transition from the 0.04 eV level to the 0.10 eV level only when $[O_i] > 10^{16}$ cm^{-3}. Also, in cases at higher diffusion temperatures (1040°C, instead of 900°C), all shallow trap levels could be suppressed. These results are summarized in the four cases shown in Fig. 6. Figure 6 also indicates that we believe that these shallow states communicate in some way with deeper mid-gap states, but little can be said about this at this time.

The results suggest that some sort of oxygen-related complex is formed at these electrically active dislocations. The complex then dissolves or breaks up when T > 1040°C. For $[O_i] > 10^{16}$ cm^{-3}, there is an interaction with the

shallowest trap at $E_c - 0.04$ and traps at $E_c - 0.10$ and $E_c - 0.13$ eV then manifest themselves. The effect of carbon in all this remains to be uncovered, but since carbon is present in concentrations of the order of 10^{18} cm^{-3}, it probably has a major role to play.

Recently, we have begun using low temperature EBIC to study dislocations which are formed under known stress and temperature conditions. In order to establish a reference, initial work has been done on single crystal material. The utility of low temperature EBIC in enhancing recombination at the dislocations formed in this case by plastic deformation can be seen in Fig. 7. Shallow trap levels have not yet been measured here but the highly enhanced low temperature EBIC contrast of these dislocations is quite evident from Fig. 7.

Diffusion Length and Surface Recombination Velocity Measurements

The inhomogeneous distribution of the two types of defects which are easily imaged by EBIC, namely dislocations and grain boundaries, means that the diffusion length, L, also varies spatially in material which contains these defects.

In analyzing the current collection in EBIC when defects or regions of diminished values of L are present, several approaches are possible. One approach is to treat the defect as a perturbation such that L changes abruptly when a defect is encountered. With this approach to the problem, an analysis built up using point defects can be done so that line defects and planar defects can be studied. Donolato [5] has used this method extensively in his papers and we will show how it can be utilized further on in this section.

An approach which represents an opposite extreme can also be taken [4] where one assumes (1) that the defects are distributed over a finite volume and in fact fill the generation sphere, and (2) that L varies in a smoother and less abrupt fashion in moving from a defect to a defect-free region.

Both of these approaches will be illustrated with experimental examples which will also show the advantages and disadvantages of each approach.

The shallow trapping level model utilized in the interpretation of the low temperature EBIC data implicitly used the second approach where the defect is visualized as filling the generation sphere. This, of course, is a simplistic assumption but it allows us to assign a number or diffusion length at any particular point along an EBIC line scan. Figure 8 shows EBIC micrographs of the same region of a sample of EFG silicon ribbon before and after thermal processing. In Fig. 9 are shown line scans through the same region before and after thermal processing along with the decrease in diffusion length values at various points following the thermal processing. The recombination seen after the thermal processing occurs at the same sites which exhibit enhanced recombination at low temperatures. This type of data as well as the low temperature EBIC data leads to a picture of the intragranular dislocation arrays as being the sites at which recombination changes take place, including changes in the shallow electron traps.

The first approach to measuring L, that used by Donolato [5], allows one to measure a surface recombination velocity, S, at a given boundary as well as

the diffusion length for intragranular regions on either side of this boundary. One takes a line scan through the grain boundary and by measuring simple geometric properties of the line scan related to the half width, these parameters can be extracted. This method is more accurate than the one described above, but requires a relatively "clean" boundary without extremely dense dislocation arrays adjacent to it, a situation which is often found in silicon ribbon. In the following section on hydrogen passivation, an application of this method will be described.

Hydrogen Passivation

In the early work on hydrogen passivation of grain boundaries, it was demonstrated that the electrical properties of grain boundaries could be dramatically altered after hydrogen passivation [6]. This was a perfect application for EBIC, and, in fact, dramatic before and after EBIC photos of hydrogen passivation of grain boundaries were obtained [7], along with impressive improvements in solar cell efficiency.

An example is shown in Fig. 10. EBIC photos such as these indicated that in some cases hydrogen passivation could virtually eliminate any EBIC contrast due to grain boundary recombination. These EBIC photos were made at 30 keV, where R ~ 9 μm. Thus, passivation proceeded down to this depth, but did it proceed any further?

To answer this question, a technique was developed to measure the depth of penetration of hydrogen passivation down grain boundaries [8]. Figure 11 is an illustration of the configuration used. The sample is cleaved and the cleaved surface is exposed to hydrogen ions. A blocking layer of PH_x diffusion-produced glass subsequently covered with a thin layer of evaporated Ti is used to confine the hydrogen penetration to be normal to the cleaved surface. After passivation, the sample is turned 90° and EBIC is done on the side with the blocking layer. The Ti layer is thin enough to permit penetration of the electron beam. A typical result obtained with this technique is shown in Fig. 12. In this way, passivation depths of anywhere from ~5 μm to ~200 μm were found. This variation was due to great differences in the recombination properties of different boundaries. Using the method of Donolato, referred to above, to measure S, a roughly linear relationship for ln S vs. the passivation depth, x, was found for $x \leq 35$ μm and $S \geq 2 \times 10^4$ cm²/sec. This is shown in Fig. 13.

Exploiting this technique even further, it was found that diffusivities of hydrogen down grain boundaries could be measured at 400°C and ranged from 10^{-8} to 10^{-10} cm²/sec. These values were the first direct diffusivity measurements of hydrogen diffusion down grain boundaries and show the power of EBIC in better understanding hydrogen passivation.

Summary

The utility of EBIC in studying recombination in silicon ribbon has been described. Efforts at quantifying the technique have begun to yield some fruit. The behavior of shallow electron trapping levels associated with dislocations in the material has been monitored. The situation, while undoubtedly complex, does show that there are three basic traps and that they are especially sensitive to

[O_i] and thermal processing. Thus, the method could be of use in better understanding the role of oxygen and thermal processing in this material. The use of low temperature EBIC in studying these traps, and, in general, in studying the electrical behavior of dislocations has been discussed.

Hydrogen passivation of defects in silicon ribbon is a particularly apt application of EBIC analysis. EBIC work has already shown that passivation depths can vary from 5 to 200 μm along grain boundaries and that hydrogen diffusivities along such boundaries can vary from 10^{-8} to 10^{-10} cm^2/sec.

References

1. J.I. Hanoka and R.O. Bell, Ann. Rev. Mater. Sci., 11, 353 (1981).

2. J.I. Hanoka, Solar Cells, 1, 123 (1979/80).

3. J.I. Hanoka, R.O. Bell and B. Bathey, in: Proc. of Symposia on Electronic and Optical Properties in Polycrystalline or Impure Semiconductors and Novel Silicon Growth Techniques, ed. by K.V. Ravi and B. O'Mara, The Electrochem. Soc., Princeton, 1980.

4. R.O. Bell and J.I. Hanoka, J. Appl. Phys., 53, 1741 (1982).

5. C. Donolato, Appl. Phys. Lett., 34, 80 (1979), and C. Donolato, Scanning Electron Microsc., Part I (1979), p. 257; also, C. Donolato and R.O. Bell, Rev. Sci. Instrum., 54(8), 1005 (1983).

6. C.H. Seager and D.S. Ginley, Appl. Phys. Lett., 34, 5 (1979).

7. J.I. Hanoka, C.H. Seager, D.J. Sharp, and J.K.G. Panitz, Appl. Phys. Lett., 42(7), 618 (1983).

8. C. Dubé, J.I. Hanoka, and D.B. Sandstrom, Appl. Phys. Lett., 44(4), 425 (1984).

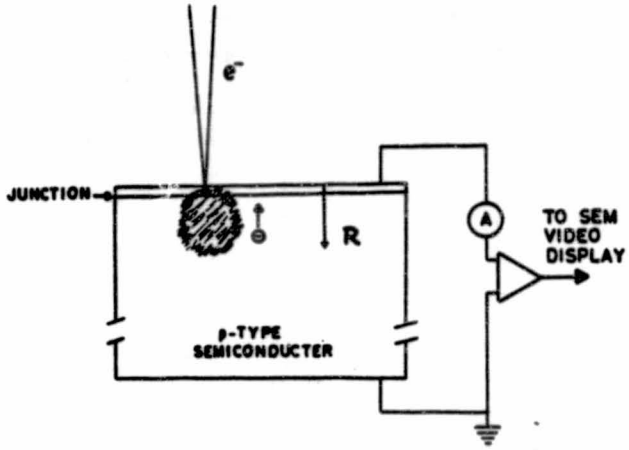

Fig. 1. Schematic of the EBIC process. Electron-hole pairs are generated within the shaded region. In the p-type region, electrons diffuse to the junction, are collected, and then form the beam-induced current.

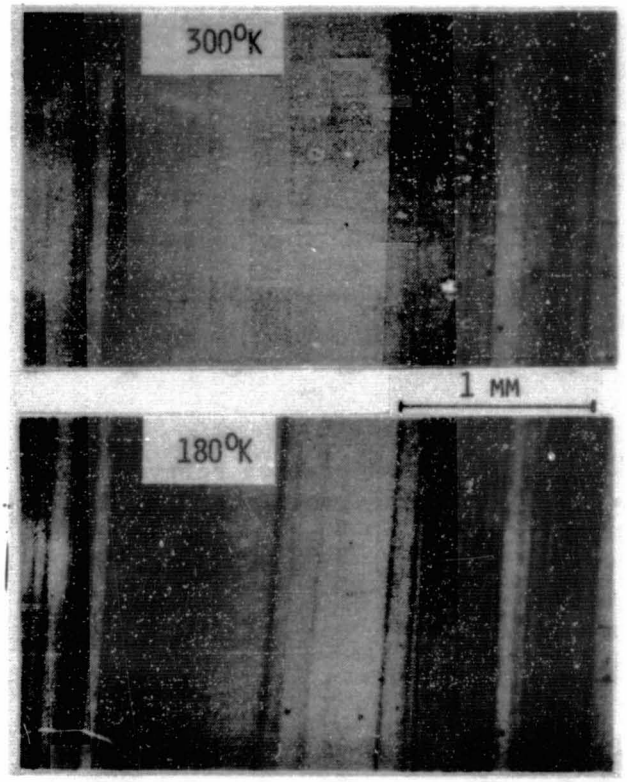

Fig. 2. Room temperature (top) and low temperature EBIC (lower photo) of the same region. Direction of growth of the ribbon is vertical.

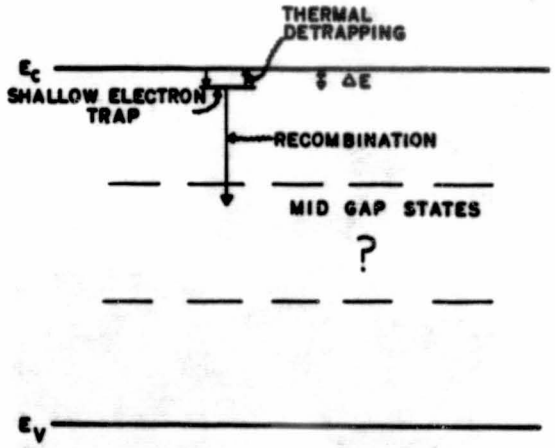

SCHEME FOR SHALLOW TRAPPING MODEL

Fig. 3.

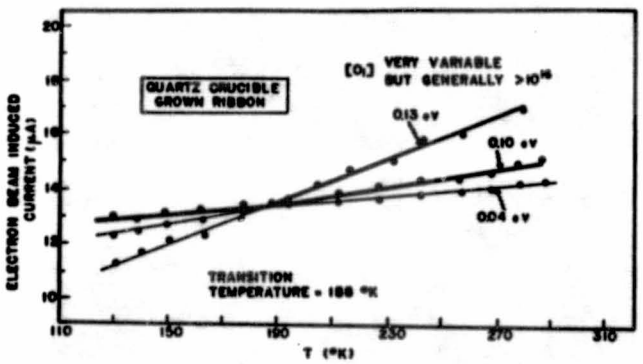

Fig. 4. EBIC temperature behavior for quartz crucible-grown ribbon.

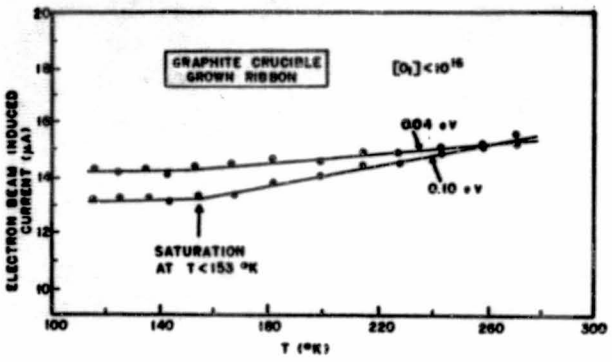

Fig. 5. EBIC temperature behavior for graphite crucible-grown ribbon.

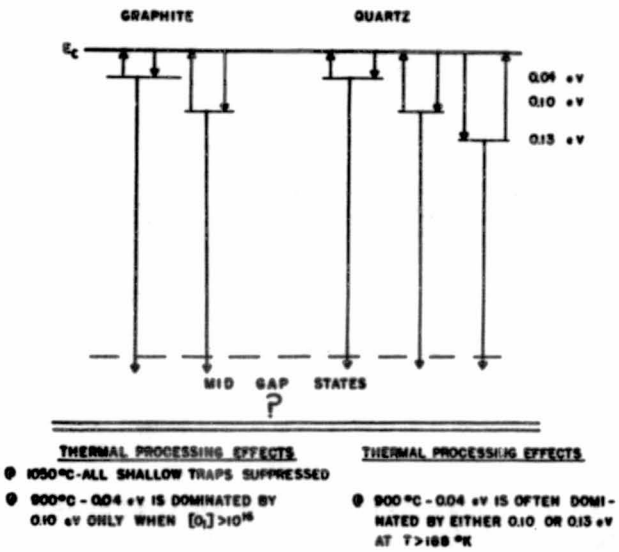

Fig. 6. Summary of shallow trap behavior.

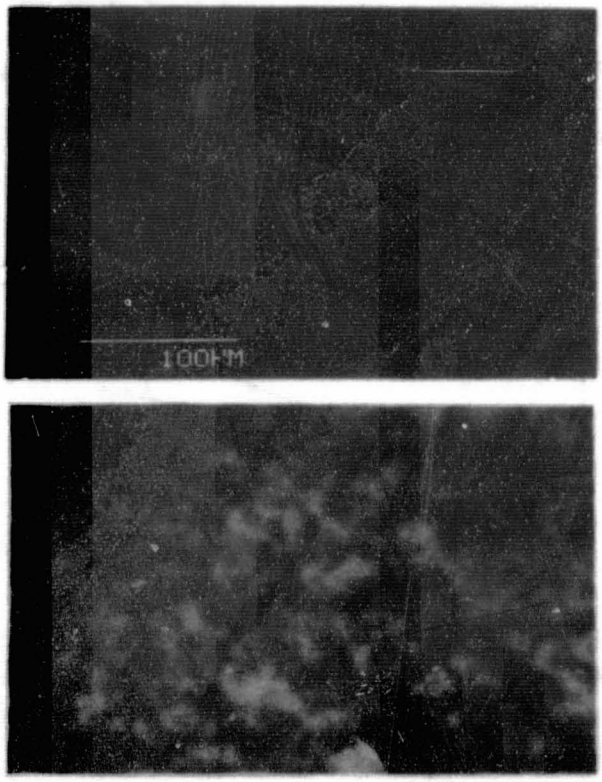

Fig. 7. Dislocations in CZ single crystal sample stressed at 1300°C using four-point bending. Top: room temperature; bottom: 150°K.

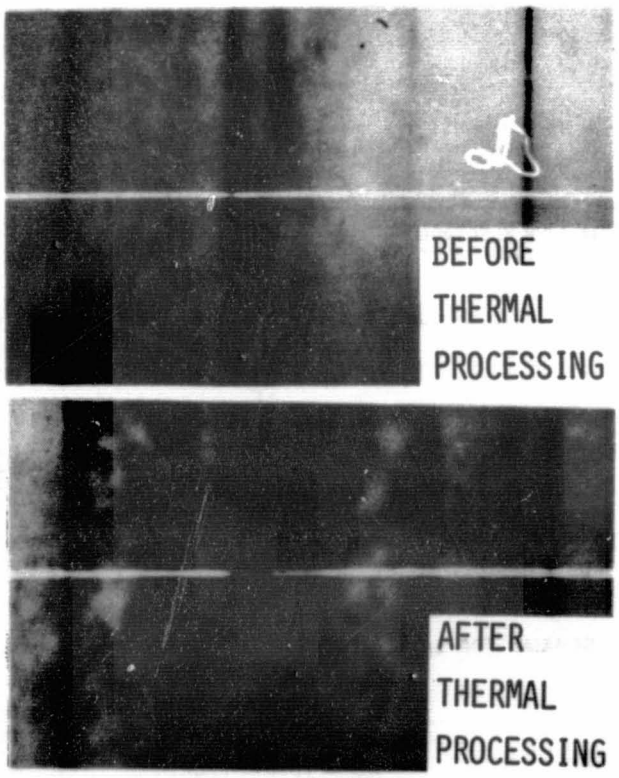

Fig. 8. EBIC micrographs of the same region before and after thermal processing.

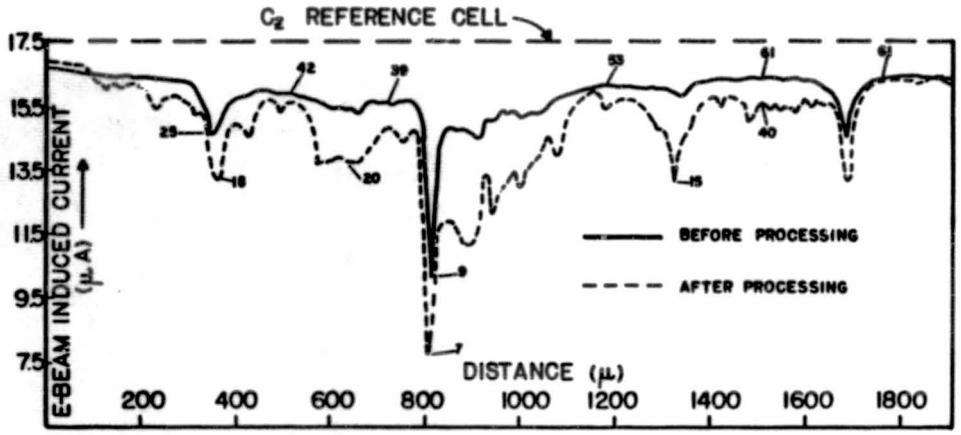

Fig. 9. Line scans for the two cases in Fig. 8.

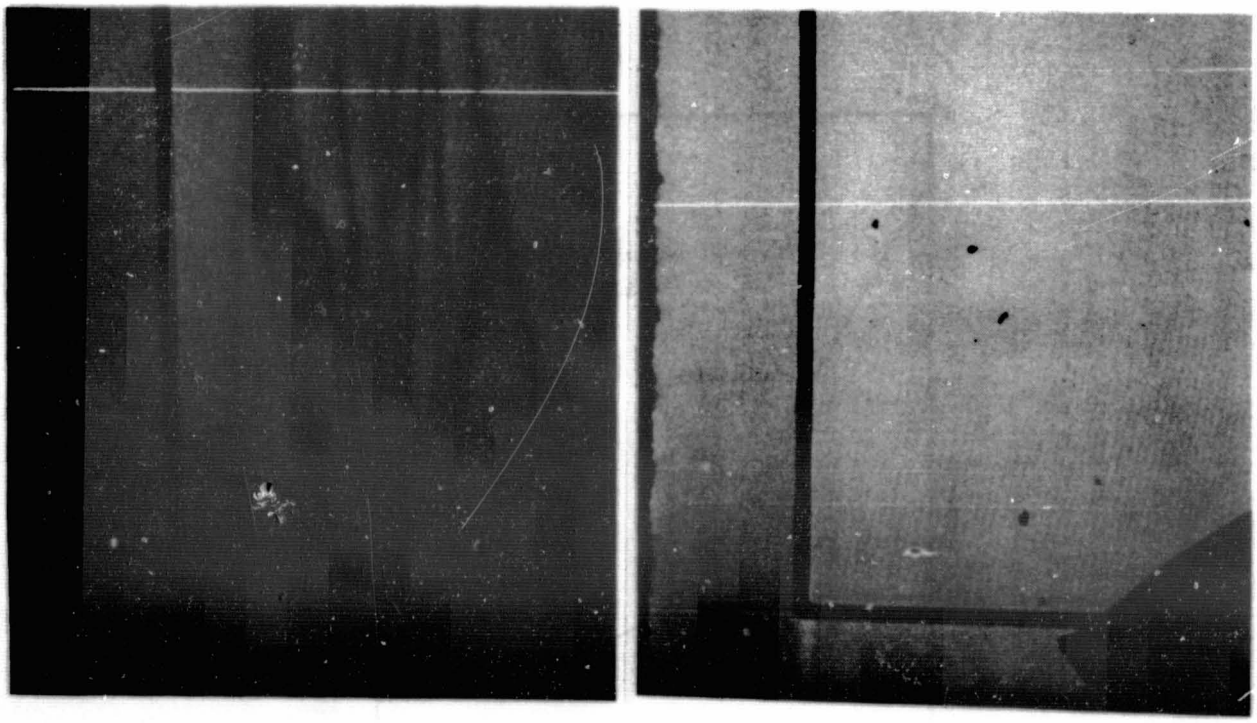

Fig. 10. EBIC photos of a ribbon solar cell before and after passivation.

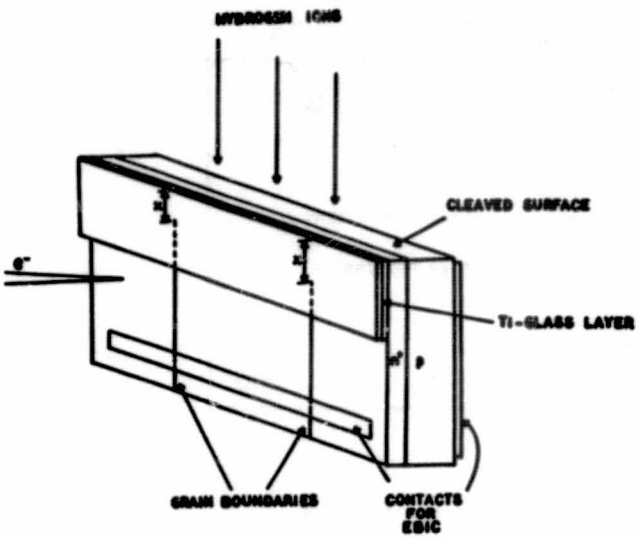

Fig. 11. Scheme used for passivation depth measurements.

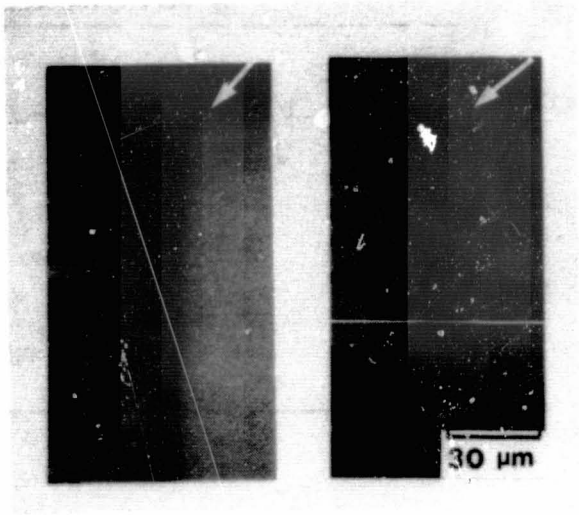

Fig. 12. Passivation depths using the technique of Fig. 11.

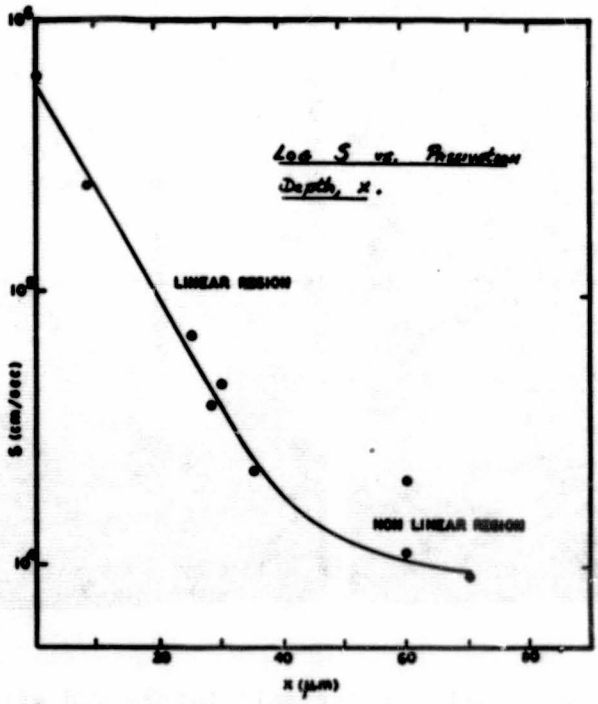

Fig. 13. Relation between surface recombination velocity S and passivation depth, x.

DISCUSSION

ROHATGI: When you showed the diffusivities of 10^{-8} to 10^{-10}, I take it you are saying that this is the diffusivity in the grain boundaries, but not necessarily in the bulk silicon.

HANOKA: That is right.

ROHATGI: You also indicated that you think that hydrogen went in the bulk, also through one of your measurements. Did I read you right?

HANOKA: That is right.

ROHATGI: How deep was the detection of the hydrogen?

HANOKA: In fact, it is not something I am discussing here, but we have a considerable amount of evidence to indicate that the hydrogen goes down in the bulk rather deeply also. We will be publishing some data on that very soon.

ROHATGI: This is in contrast to what Larry (Kazmerski) said in his talk this morning, that hydrogen doesn't go through the bulk silicon.

HANOKA: It is not a simple bulk diffusion. Through ordinary good non-defect-free silicon, because there isn't much data on the diffusion of hydrogen down bulk silicon, but data indicate that the diffusivities are something like 10^{-14}, so you don't expect -- it's only Angstroms that you would expect the hydrogen to be going that way. So it has to be a defect-assisted diffusion down the bulk region.

ROHATGI: Then I take it this range of 10^{-8} to 10^{-10} that you had was based on this range of passivation that you saw all the way from 5 to 100 micometers.

HANOKA: Yes, that is right.

ROHATGI: That is the reason for this big range?

HANOKA: Yes. Generally, the boundaries that show the shallowest passivation are the one that have the highest surface recombination velocity.

LESK: Can you please mention your beam current densities and whether or not you had attempted to control the temperature during the implant?

HANOKA: The current densities were about 2 milliamps/cm^2 and the temperature -- it is hard to measure the temperature and there is some controversy about this -- but I think the temperatures of our samples are fairly high, something on the order of 400°C to 500°C when we passivate.

DAUD: Could you comment about your numbers for the diffusion length? If the distance between the grain boundaries is less than the diffusion length in this area, is your measurement correct?

HANOKA: You are probably right but generally what you find is the distance between the electrically active boundaries on the order of several hundred micrometers on average, and our diffusion lengths unfortunately are not several hundred micrometers. So I don't think that is a problem in most cases.

SIRTL: You mentioned these trap levels, and particularly the one correlated with oxygen. Is this something that has been reported the first time by you?

HANOKA: Actually, I gave it at the ECS meeting in Minneapolis about two or three years ago, but I have not published it. It was just an oral presentation, but I am planning to publish it soon.

SIRTL: So far nobody else has.

HANOKA: Not that I am aware of.